diffusion-fundamentals

The Open-Access Journal for the Basic Principles of Diffusion Theory, Experiment and Application

Water self-diffusion studies in complex materials with fast-relaxing components: Static and pulsed field methods revisited

Achim Gädke[1], Karen Friedemann[2], Petrik Galvosas[2], Frank Stallmach[2], Jörg Kärger[2], Nikolaus Nestle[1,3]

[1] TU Darmstadt, Institute of Condensed Matter Physics, Darmstadt, Germany
[2]Universität Leipzig, Abteilung Grenzflächenphysik, Leipzig, Germany
[3]Present adress: BASF AG Ludwigshafen, Germany

Corresponding author: Nikolaus Nestle, TUD-IFP, Hochschulstraße 6, D-64289 Darmstadt, Germany, E-Mail: nikolaus.nestle@physik.tu-darmstadt.de

(received 4 April 2007, accepted 3 June 2007)

Abstract

Field gradient NMR techniques have proved very useful for measurements of molecular self-diffusion coefficients in many materials ranging from simple liquids to more complex materials such as polymer melts, porous media and biological tissues. In such multicomponent systems, spin relaxation phenomena may not only lead to a reduction of the signal intensity available for the field gradient NMR experiment but also to systematical errors in the measured diffusion coefficient due to unwanted relaxation time weighting. While pulsed field gradient (PFG) techniques allow better separation of relaxation and diffusion effects, they require at the same time longer echo times. This in turn aggravates unwanted weighting by transverse relaxation. For materials containing fast-relaxing components such as clayey sediments or partially hydrated cement the use of static field gradient (SFG) techniques suggests substantial benefits due to shorter echo times (i.e. less transverse relaxation time weighting). However, the separation of relaxation and diffusion effects is more difficult in SFG. In this contribution, we present the echo ratio approach to separate both effects and discuss its limitations. As we will show on the basis of experimental and calculated results, the echo ratio technique works well for homogeneous samples and complex materials with sufficiently long longitudinal relaxation times. In materials with components for which T_1 is comparable or shorter than the diffusion time, however, this approach also fails and no meaningful interpretation of the SFG data on the basis of simple fit functions is possible so far.

Keywords

SFG NMR diffusometry, ultrastrong gradients, cement, hydration, relaxation-time-filtering

1. Introduction

Field gradient NMR provides a unique tool for studies of molecular self-diffusion coefficients, at it allows a transient and non-invasive position labeling of diffusing molecules. In particular,

- no cumbersome application of tracer substances (chemically or isotopically marked) is needed,
- real self-diffusion coefficients without any concentration gradient are achieved and
- it is possible to measure diffusion coefficients at different diffusion times (under favourable conditions in the range from about 1 ms to several seconds) and to analyze diffusion coefficients as a function of the reciprocal diffusive shift [1].

The impact of diffusion in magnetic field gradients on excited NMR magnetizations has first been reported by Erwin Hahn in his first paper on spin echoes [2]. The first application of the diffusion effect in static field gradients for NMR diffusion measurements was reported a few years later [3]. Further milestones in the development of NMR diffusometry were the introduction of the pulsed field gradient spin echo technique [4] and the stimulated echo pulsed field gradient method [5]. Reviews on the present stage of NMR diffusometry can be found in [6,7,8,9,10].

While diffusion measurements in simple liquids [6,7,11], in some regular porous media such as zeolites [8] and in certain fields of medical MRI [12] have reached remarkable levels of precision, the application of field gradient NMR to many more irregular natural and technical multicomponent materials (such as sediments, biofilms, hydrating cement or many types of biological tissues) is complicated by relaxation time weighting effects.

In the further course of this paper we will first shortly review the effect of spin relaxation on standard stimulated echo PFG and SFG experiments for simple and multicomponent materials. The echo ratio approach for eliminating T_2 effects in stimulated echo SFG experiments will be described. After that, we will illustrate the typical problems arising from relaxation time weighting on the basis of magnetic field gradient diffusometry results obtained on hydrating cement pastes. After this, the effect of longitudinal relaxation on the echo ratio in the SFG experiment will be further demonstrated on the basis of some simulated magnetization decay curves and conclusions for the applicability of echo ratio SFG NMR to multicomponent materials will be drawn.

2.Materials and Methods

The spectrometer setup for SFG was essentially that described in [13] however with the new DAMARIS control software developed recently at the institute [14,15]. The multitriggering capabilities of the new spectrometer console based on this software allow the acquisition of both major echoes of a stimulated echo sequence within one run. In this setup, a solenoidal RF coil oriented perpendicular to the magnetic field direction is used. The sample was put into the coil in a way that the Teflon plugs were outside the coil in order to minimize a possible contribution of ^{19}F resonances. These contributions may arise due to the strong magnetic field gradient used in the experiment, leading to a distance of less than a millimetre between sites where resonance occurs for protons and for fluorine nuclei at the same frequency. from the Teflon to the detected NMR signal. The proton resonance frequency used in the experiments was 75 MHz, the strength of the magnetic field gradient 192 T/m. The

diffusion coefficient was determined by analyzing the ratio of the stimulated echo and the primary echo (see figure 1A) as a function of τ^2. The rationale and limitations for this approach will be discussed in section 3.

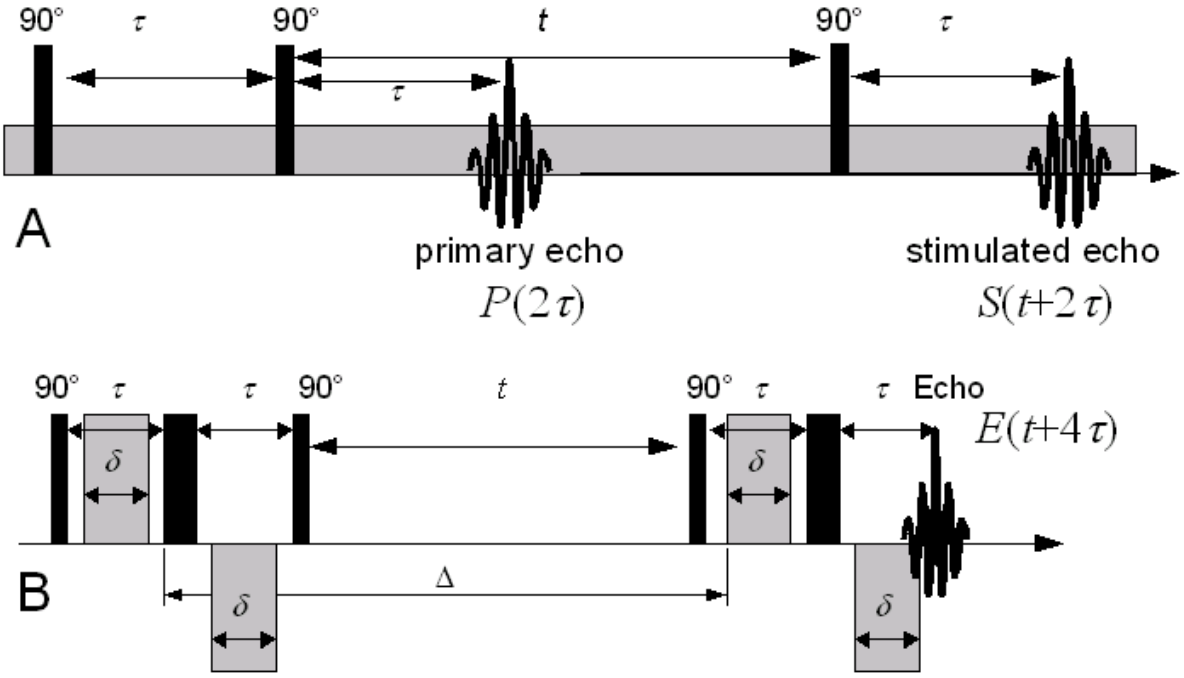

Fig. 1: NMR diffusometry pulse sequences used (A) SFG and (B) PFG experiments reported here. Gray rectangles denote gradient (pulses) and black rectangles the RF pulses

The spectrometer for the PFG experiments was the FEGRIS NT facility in Leipzig [16] which was operated at a proton resonance frequency of 125 MHz. Except for the use of this different frequency, all details of the measurement procedure were the same as described in [17]. In order to compensate the detrimental effect of internal background gradients inside the sample on the measured diffusion coefficient, the 13-interval PFG sequence [18] depicted in figure 1B was used.

The cement samples used for the example experiments were produced from commercial white cements "Aquila Bianco" CEM I 32.5 R by Cemencoll, Forlì, Italy and "Dyckerhoff weiß" CEM I 42.5 R by Dyckerhoff, Wiesbaden. Cement pastes at extremely low water/cement ratios (w/c) of 0.18 ml/g to 0.25 ml/g (without additives such as superplasticizers) were produced by means of a two stage mixing procedure:

- in a first step, the cement powder was mixed with water in a small quadratic polypropylene container by means of a PVC stirring rod. At the low water cement ratios of 0.25 ml/g, 0.20 ml/g and 0.18 ml/g used in this study, this mixture still did not produce a workable cement paste.
- in a second step, the mixture of cement powder and water was therefore put into a stamping device (made from PVC) in which cement pastes of sufficient workability could be produced by repetitive stamping and mixing of the paste.

These pastes then were filled into short (1.3 cm) pieces of thin-walled glass tube (5 mm outer diameter) which either were closed using two Teflon® plugs (for the SFG experiment) or dropped into another glass tube (for the PFG experiments [17]). The PFG experiment were started about 10 min. after mixing the paste, the SFG was started after about 1 day. The samples in both experiments were kept at room temperature (298 K ±2 K).

In the SFG experiments the echo time was varied in 60 logarithmic steps from 20 µs to 1.5 ms. In order to be able to identify possible drift effects, the echo delays were varied in an interleaved fashion. The repetition time was 0.3 s, and the diffusion time was set to 3 ms. Several 100 to 1000 averages were taken for each echo time so that measuring times on the order of several hours resulted for each SFG experiment.

3. Diffusion and relaxation effects in field gradient NMR

3.1 Homogeneous samples

For a homogeneous sample, the amplitude of the echo at the time $t+4\tau$ in the PFG experiment in Fig. 1A is given as:

$$E(t+4\tau,G) = e^{-t/T_1 - 4\tau/T_2} A_{D,A}(t,\tau,G) \qquad (1)$$

with $A_{D,A}$ denoting the echo attenuation due to diffusion

$$A_{D,A}(t,\tau,G) = \exp(-\gamma^2\delta^2G^2D(4t+6\tau-\tfrac{2}{3}\delta)) = \exp(-b_A(t,\tau,G)D) \qquad (2)$$

with $b_A = \gamma^2\delta^2G^2(4t+6\tau-\tfrac{2}{3}\delta)$.

In the experiment, b_A is varied by varying the amplitude G of the gradient pulse. Except by determining the overall signal amplitude available for the diffusion measurement, relaxation times have no influence on the diffusometry experiment.

The diffusion coefficient in this experiment is determined as the slope of a plot of ln ($E(t+4\tau$,G)) over b_A (see fig. 2).

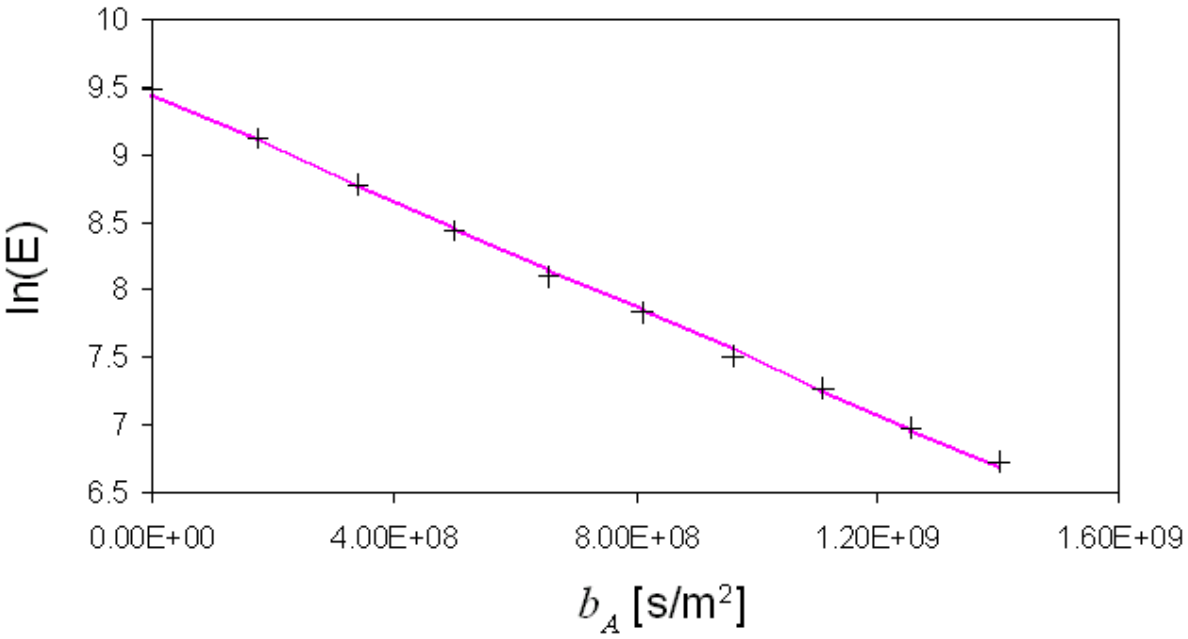

Fig. 2: Determination of the diffusion coefficient in the PFG-NMR experiment of fig. 1A as the slope in the plot of ln ($E(t+4\tau$,G)) over b_A . (Sample: egg plant fruit tissue, diffusion time 50 ms, measured diffusion coefficient at 304 K: (1.977±0.025)×10^{-9}m^2/s. For details see [19])

In contrast to the echo attenuation in a PFG NMR experiment as described by eq. (2), the echo amplitude in the SFG experiment (see fig. 1A) depends on both, the attenuation due to relaxation as well as diffusion. Thus, the two echoes $P(2\tau)$ and $S(t+2\tau)$ exhibit the following behaviour: :

$$P(2\tau) = \exp(-2\tau/T_2 - \tfrac{2}{3}\gamma^2 G^2 D\tau^3) \qquad (3)$$

and

$$S(t+2\tau) = \exp(-2\tau/T_2 - t/T_1 - \gamma^2 G^2 D\tau^2(\tfrac{2}{3}\tau + t)) \qquad (4).$$

As the gradient is static, the only options to vary the diffusion effect are variations of t and τ. As one can see from the expressions given by eq. (3) and (4), the echo attenuation due to relaxation also changes in both cases. For a diffusion experiment on the basis of the amplitude $S(t+2\tau)$ of the stimulated echo, it is therefore necessary to separate the effects of relaxation and diffusion in the analysis of the echo. For materials with sufficiently long relaxation times, the relaxation effects may just be neglected over the dominating diffusion effect. Otherwise, one has to fit the echo decay curve from eqn. (4) to the experimental signal decay curve. As both effects lead to monotonously falling signal intensity, such a fit requires very good signal/noise ratio in order to allow a numerically stable separation of relaxation and diffusion effects.

If both the amplitudes from the primary and the stimulated echo are available, this opens up two options for better separation of diffusion and relaxation effects:

- Fitting eqns. (3) and (4) simultaneously to the two echo data sets. This option requires non-linear fitting procedures which are numerically more difficult to handle than linear fits as they require well-chosen starting values and tend to be more susceptible to noise than simple linear fits.
- Separating the effect of transverse relaxation from the diffusion by evaluating the ratio of the two echoes:

$$\frac{S(t+2\tau)}{P(2\tau)} = \frac{\exp(-t/T_1 - 2\tau/T_2)}{\exp(-2\tau/T_2)} \frac{\exp(-\gamma^2 G^2 D\tau^2(\tfrac{2}{3}\tau + t))}{\exp(-\tfrac{2}{3}\gamma^2 G^2 D\tau^3)} = \exp(-t/T_1)\exp(-\gamma^2 G^2 t\tau^2 D)$$

$$= \exp(-t/T_1)\exp(-b_B(t,\tau,G)D) \qquad (5)$$

with $b_B = \gamma^2 G^2 t\tau^2$.

In the experiment, b_B is varied by varying the time τ. While the ratio S/P in eqn. 5 contains no explicit τ -dependent T_2 weighting, changing τ nevertheless leads to a change in the relaxation weighting (see eqns. 3 and 4) of both the primary and the stimulated echo (which only cancels out in the ratio of the two). A strong T_2 effect on both echoes will usually deteriorate the signal/noise ratio of the two echoes and even more so of the ratio S/P. In order to keep these problems manageable, it is especially important to avoid baseline offsets in the two echoes. This typically can be achieved by phase cycling.

The value of the diffusion coefficient in this experiment is obtained as the slope of the plot of $\ln(S/P)$ as a function of b_B (see fig 3).

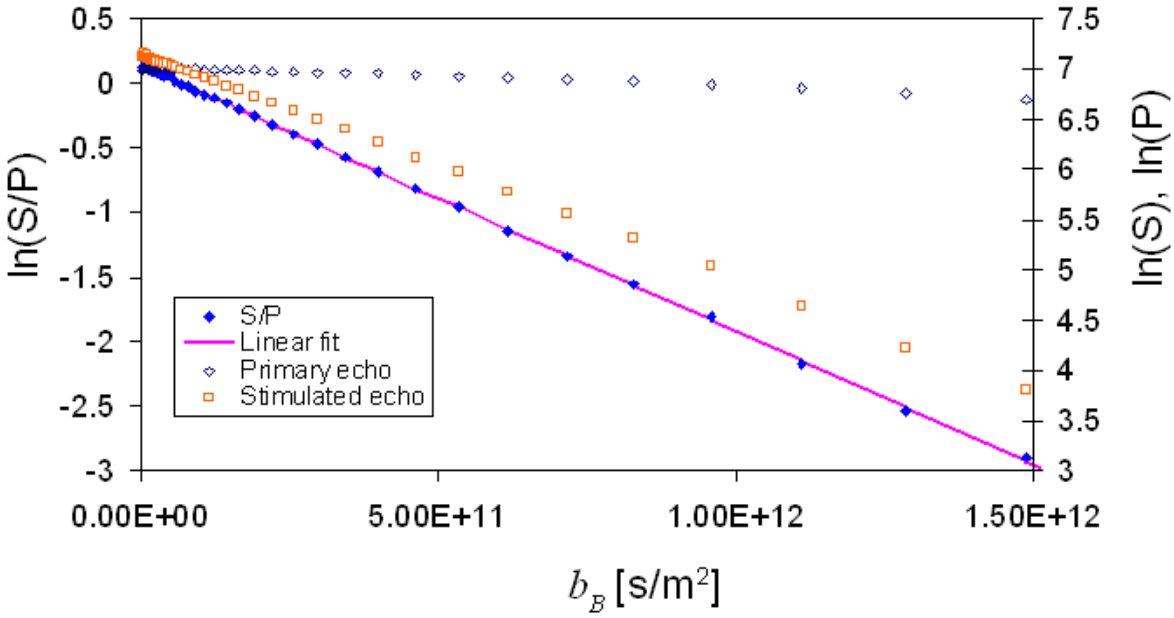

Fig. 3: Determination of the diffusion coefficient in the SFG-NMR experiment of fig. 1A as the slope in the plot of ln(*S*/*P*) as a function of b_B. In addition to the ratio of the echoes, also the primary echo and the stimulated echo are given in the plot. The resulting diffusion coefficient for a glycerol samples at 303.2 K is $(2.058\pm0.04)\times10^{-12}$m^2/s.

To summarize, the separation of diffusion and relaxation in PFG experiments on homogeneous samples is achieved as echo times are kept constant and only the amplitude of the gradient pulse is varied. In SFG experiments, the ratio *S*/*P* is not directly affected by the variation of relaxation time weighting. It may however exhibit a poor signal/noise ratio if the T_2 effect on the individual echoes is strong. As we shall see in the next section, both of these conclusions won't hold any more for multicomponent materials.

3.2 Multicomponent samples

The echo amplitude $E(t+4\tau,G)$ observed in a PFG measurement (see fig. 1A) for a multicomponent sample is the sum of the relaxation and diffusion responses of the individual components (if exchange processes between the different components can be neglected):

$$E(t+4\tau,G) = \sum_{i=1}^{N} c_i \exp(-t/T_{1,i}) \exp(-4\tau/T_{2,i}) \exp(-b_A(t,\tau,G)D_i) \qquad (6)$$

In the standard evaluation of the PFG data (as shown in fig. 2), $\ln E(t+4\tau,G)$ is evaluated as a function of b_A. As one can see from the example data set for a complex material in fig 4, the initial part of this signal attenuation curve can be approximated by a linear function (which can again be evaluated by means of linear regression analysis).

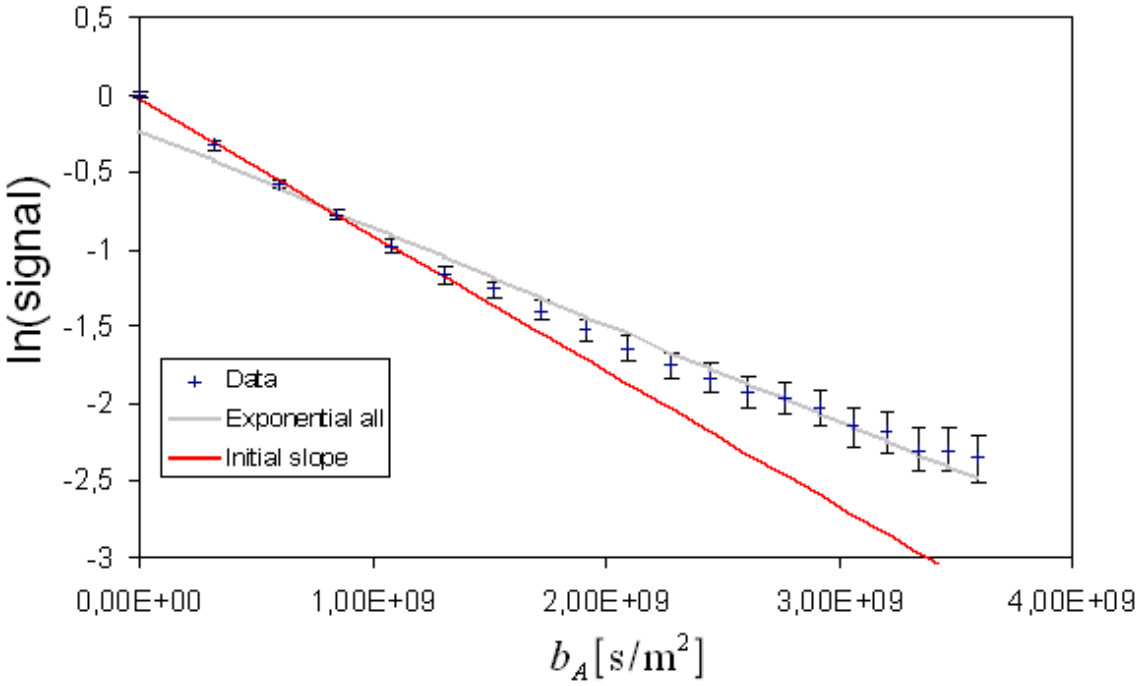

Fig. 4: Echo attenuation curve obtained in a PFG NMR experiment on a white cement sample w/c 0.25 after about 4 h of hydration. The data set was recorded using the 13-interval sequence (fig. 1B) with an echo time of 320 µs, a gradient duration of 170 µs and a diffusion time of 3 ms. Note the non-exponential nature of the echo attenuation curve: the correlation coefficient in the curve fitted to all data points is 0.982, the one in the fit of the initial slope (first 6 data points) is 0.998.

The physical meaning of the slope determined in this analysis can be calculated by developing $\ln E(t+4\tau,G)$ into a Taylor series:

$$\ln(E(t+4\tau,G)) \approx E(t+4\tau,0) - \left(\frac{\sum_{i=1}^{N} c_i \exp(-t/T_{1,i}) \exp(-4\tau/T_{2,i}) D_i}{\sum_{i=1}^{N} c_i \exp(-t/T_{1,i}) \exp(-4\tau/T_2)} \right) b_A + O(b_A{}^2) \qquad (7)$$

The linear term in this Taylor expansion (which corresponds to the initial slope of the graph in fig. 4) describes the Relaxation-Weighted Mean Diffusion coefficient (RWMD) [17]. One has to be aware that this quantity is not as representative for the transport properties of the sample as a "real" mean diffusion coefficient (without relaxation weighting) would be. Contributions of sample components with $T_{1,i} << t$, and/or $T_2 << \tau$ will just be "lost" to the diffusion coefficient in this case. Contributions of components with relaxation times in the same order as t or τ will be weighted less than their actual concentration in the sample.

Relaxation time weighting also takes place for the ratio between the stimulated and the primary echo. Instead of the simple expression for S/P in equation 5, we now end up with the expression

$$\ln\left(\frac{S(t+2\tau)}{P(2\tau)}\right) = \ln\left(\frac{\sum_{i=1}^{N} c_i \exp(-t/T_{1,i}) \exp(-2\tau/T_{2,i}) \exp(-\gamma^2 G^2 D_i t \tau^2 (1+\tfrac{2}{3}\tau/t))}{\sum_{i=1}^{N} c_i \exp(-2\tau/T_{2,i}) \exp(-\tfrac{2}{3}\gamma^2 G^2 D_i \tau^3)} \right) \qquad (8)$$

Developing this expression into a simple Taylor series in b_B is not possible in the general case. Only under the assumption that T_1-weighting can be neglected, i.e. for $T_{1,i} >> t$, it can be shown by a computation analogous to the one for the PFG case that the initial slope in the plot of the $\ln(S(t+2\tau)/P(2\tau))$ over b_B corresponds to the mean diffusion coefficient again. For the analysis of the initial slope in the presence of notable T_1-weighting, the initial slope of the plot can be analysed most easily by means of numerical simulations.

In figure 5, such simulations for ln (S/P) as a function of b_B are given for two-component-samples with various combinations of relaxation times and diffusion coefficients.

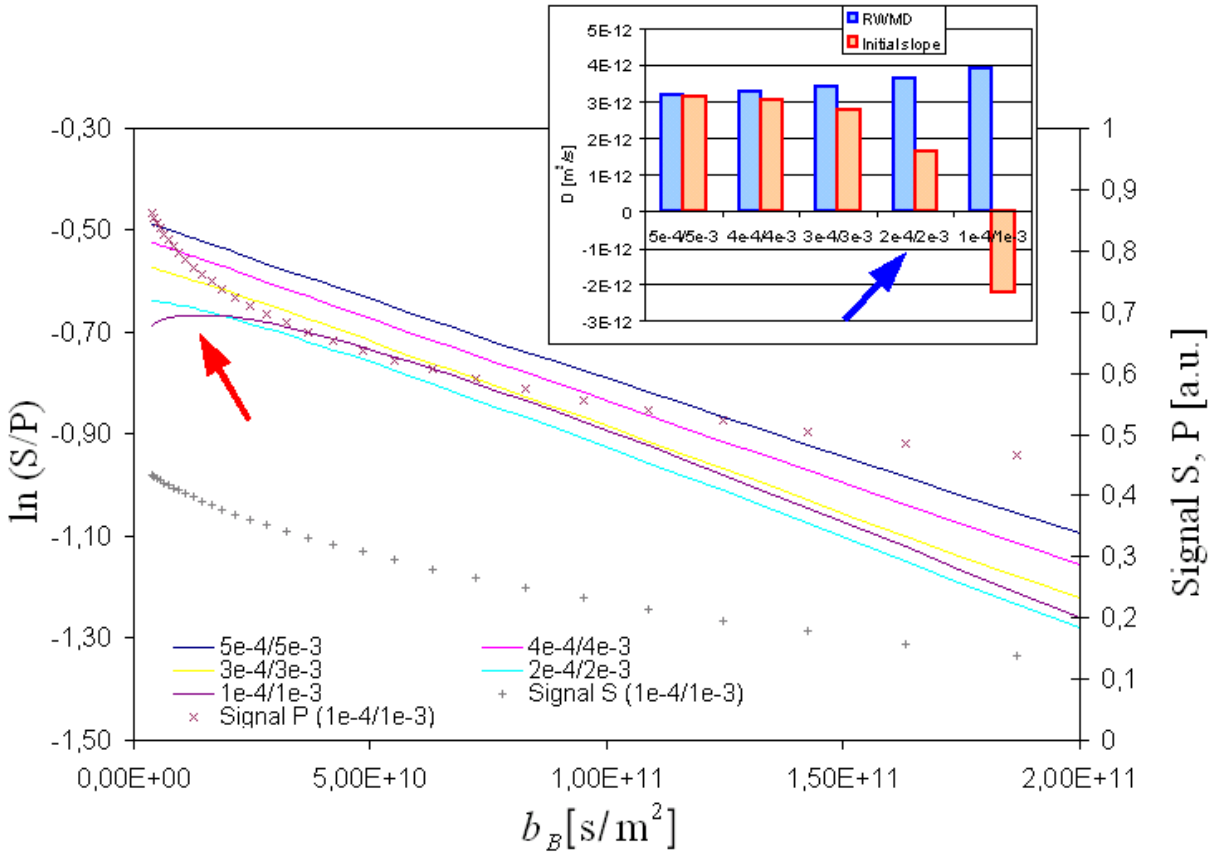

Fig. 5: Simulated behaviour of the S/P-ratio (G=192T/m, t=3ms) in a sample consisting of two components: 70% with $D = 4\times10^{-12}$m^2/s, $T_2 = 7\times10^{-4}$ s, $T_1 = 7\times10^{-3}$ s and 30% with $D = 1\times10^{-12}$m^2/s and the combinations of T_2 and T_1 denoted in the graph. In the inset, the true RWMD and the diffusion coefficients determined from the initial slopes of the ratio S/P are given. Note the flattening of the initial slope (blue arrow in the inset) and finally the change to an obviously unphysical negative diffusion coefficient for the sample with the shortest relaxation times (red arrow in graph). On the secondary axis in the graph, the amplitudes of the primary and the stimulated echo for the fastest-relaxing component are given.

As one can see from the figure, the presence of a component with short relaxation times may spoil the results of the diffusometry experiment completely. In the most obvious case, the unwanted relaxation-time weighting may lead to a positive slope in the plot (which would correspond to a negative self-diffusion coefficient in the evaluation according to eqn. 5), otherwise too low, positive self-diffusion coefficients may result from this evaluation.

Experimental examples for both cases will be provided in the next section of the paper.

4. Examples from hydrating cement samples

As already mentioned in the introduction section, hydrating cement is one of the more challenging samples for NMR diffusometry. While the first NMR diffusometry data on hydrating cement model materials have been published already nearly 30 years ago [20], it was only much more recently that diffusion in real cement samples was studied [9,17,21]. Furthermore, a wealth of profiling NMR data is available on moisture transport in hydrating and hydrated cement under unsaturated conditions [22,23]. As the changing water content in such moisture transport studies, it is limited to late hydration stages or to studies of the impact of partial drying on the hydration process. In order to study the diffusion behaviour of water during an undisrupted hydration process, field gradient NMR diffusometry is therefore the only valid approach.

The more recent NMR diffusometry experiments on hydrating cements were carried out using the PFG method shown in fig 1A on freshly prepared cement pastes during the first day of hydration [17] or on cement pastes pastes produced with a very high water/cement ratio [21]. For longer hydration times and/or lower water/cement ratios, relaxation time filtering becomes more and more of a problem, and both the quality of the diffusion measurement and its representativity for the actual diffusion properties of the water inside the cement paste become increasingly poor. This leaves a long gap between the applicability of NMR diffusometry and isotope tracer techniques [21,24] which are essentially limited to late hydration stages.

The problems arising in PFG NMR diffusion studies on cement samples at longer hydration times can be seen from figures 6 and 7:

In figure 6, diffusion coefficients (measured by PFG-NMR) of water in a hydrating sample of hydrating white cement (Dyckerhoff weiß, w/c 0.25 ml/g) are shown as a function of the hydration time. During the first 5 hours, the diffusion coefficients measured at all diffusion times exhibit only minor errors and no dependence on the diffusion time can be observed. At longer hydration times, the experimental errors in the determination of the diffusion coefficients become increasingly large as both the transverse and the longitudinal relaxation times of the water in the cement paste decrease. As measurements with longer diffusion times are more sensitive to the longitudinal relaxation time than those at shorter diffusion times, the maximal diffusion times for which meaningful diffusion coefficients can be determined become smaller and smaller with increasing hydration time. After about 1 day, even the error in the diffusion measurement at 3 ms becomes too large for meaningful data.

In addition to the increasing experimental errors (which are partially just due to the decrease in available signal intensity for the PFG experiment, see thin lines in fig. 6), the increasingly implausible dependence of the diffusion coefficient on the diffusion times (see black arrows in fig. 6) indicates the more fundamental problem of relaxation time weighting. In the absence of relaxation time weighting, the measured diffusion coefficient in a tortous medium such as a cement stone matrix tends to decrease with increasing mean diffusive shift length (i.e. increasing diffusion time). As can be seen from figure 6, this is not any more the case for the data obtained after more than 8 hours of hydration time.

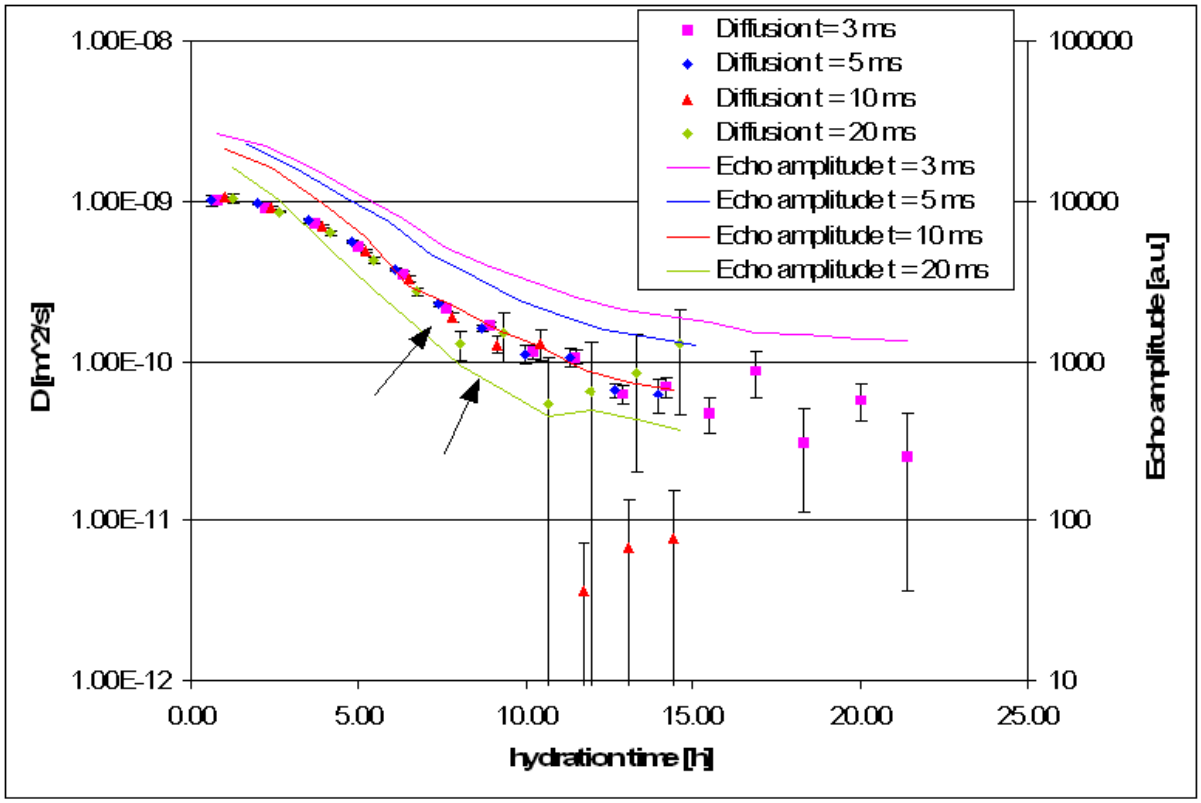

Fig. 6: Diffusion coefficients determined by PFG NMR as a function of the hydration time and for diffusion times (symbols, left axis) and the corresponding amplitudes of the echo in absence of a gradient (lines, right axis). After about 8 hours of hydration (arrows), the diffusion measurement for the two longer diffusion times is beginning to be affected more and more by relaxation-time filtering.

Figure 7 illustrates yet another problem in the determination of diffusion coefficients in hydrating cement: While the range of b_A values needed to achieve a sufficient echo attenuation for a reliable diffusion measurement is quite small for the large diffusion coefficients measured in the beginning of the experiment, the smaller diffusion coefficients at later hydration stages require a larger range of b_A to achieve evaluable echo attenuations. Figure 7 shows that the diffusion coefficients determined from evaluations of the experimental data over different ranges of b_A actually are different. The reason for those different diffusion coefficients resulting from the different evaluations can be seen in figure 4: Due to the distribution of different diffusion coefficients in the hydrating cement paste, the echo attenuation curve shows no simple exponential decay, and the slopes determined in a linear regression over different ranges of b_A will result in different diffusion coefficients.

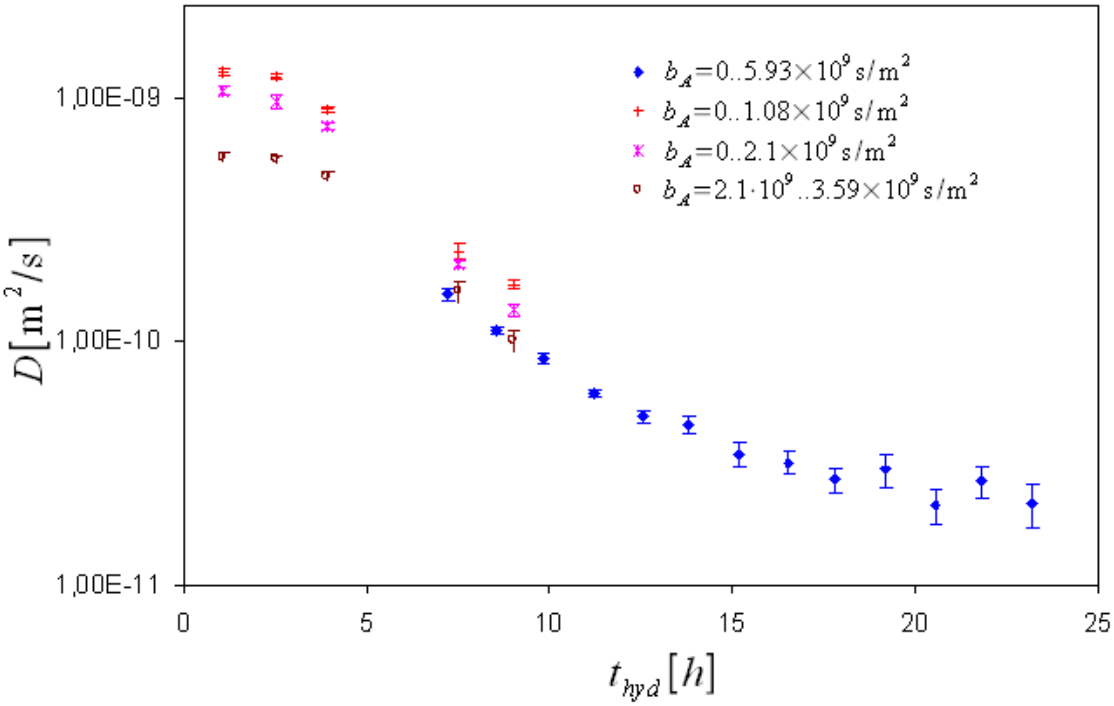

Fig. 7: Diffusion coefficients (diffusion time: 3 ms) in a hydrating cement matrix with w/c 0.25 determined by PFG NMR using different ranges of b_A . The systematically lower diffusion coefficients for wider ranges of b_A are the result of the increasing influence of slow-diffusing components in the paste.

Both the higher gradient strengths [13] and the shorter echo times (corresponding to less filtering due to transverse relaxation) available in static field NMR diffusometry seem to be favourable for diffusometry on cement pastes after a few days of hydration. Therefore, we have conducted a series of SFG experiments using the echo ratio approach described in section 3.

In figure 8, the PFG results already shown in figure 7 are given along with those from the SFG experiments measured at another white cement paste prepared with the same water/cement ratio. The jump from the "magenta" PFG data to the "blue" PFG data set in figure 8 has already been discussed in the contexts of figure 7. The jump from the "blue" PFG data to the "black" SFG data is even more dramatic. A major reason for this is the much bigger range of b_B values covered in the SFG experiment which goes from 3.7×10^9 to 4×10^{11}s/m^2 , while the maximal range of b_A values covered in the PFG experiments shown in Figs. 6 and 7 was 0 to 5.93×10^9 s/m^2. The smallest b_B value available in the SFG experiment is dictated by the echo time and the gradient strength. Extracting a diffusion coefficient from the SFG data over a much smaller range of b_B is furthermore not possible at the present signal/noise ratio in the SFG experiment. Achieving comparably high values for b_A in a PFG experiment is also not possible due to the lower gradient strengths and limited gradient durations.

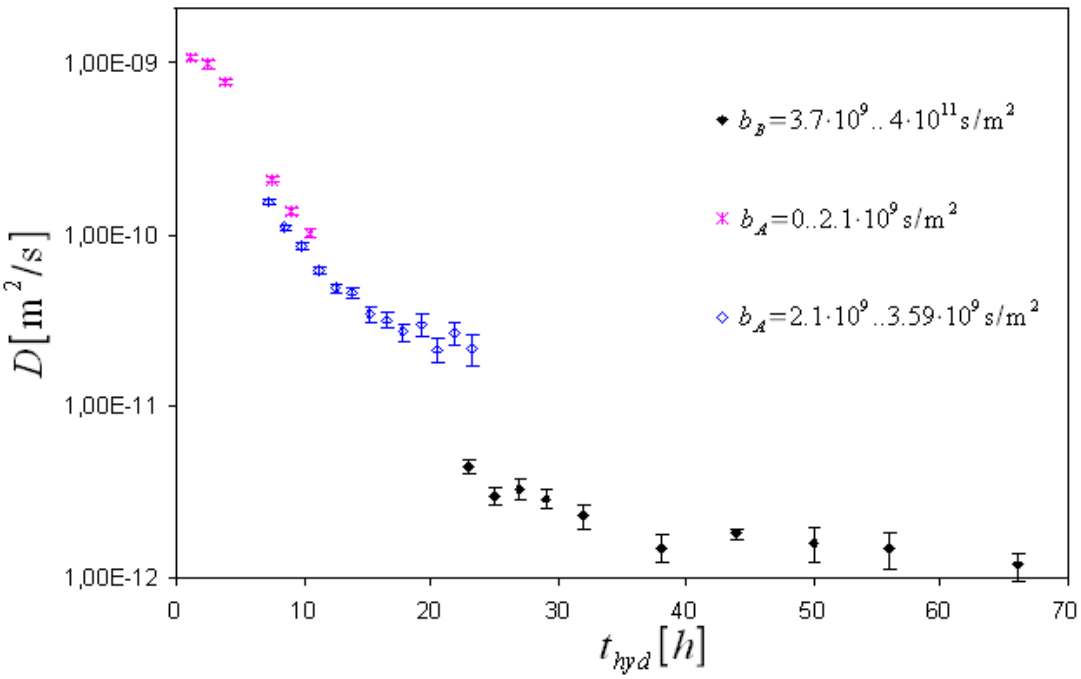

Fig. 8: Diffusion coefficients in a hydrating cement matrix with w/c 0.25 determined by PFG and SFG NMR As a result of the much wider range of b_B, the jump in the data upon the transition between PFG and SFG data is even more dramatic as the differences between PFG experiments covering different ranges of b_A.

Another reason for the very low diffusion coefficients resulting from the SFG experiments might be the sensitivity of the echo ratio to combined longitudinal and transverse relaxation effects discussed already in section 3.2.

In figure 9, the primary and stimulated echoes recorded on the sample after 34 h of hydration are given along with the echo ratio and a linear fit over the whole range of b_B values. While the overall signal/noise ratio of the echo ratio is not too good, one nevertheless can see no indications for the problems demonstrated in figure 5. Rather, the initial slope of the echo attenuation curve at small b_B values seems to be bigger than the slope for larger b_B values. This behaviour is most probably due to the distribution of different diffusion coefficients already discussed in the context of the PFG data shown in figure 4. At this intermediate hydration time the SFG experiment still provides an adequate indication on the diffusion coefficient inside the hydrating cement paste.

Figure 10, by contrast, shows the ratio of primary and stimulated echo as it is observed after 4.5 days of hydration in the same sample: The data for small values of b_B show no clear trend and even a slightly positive slope in the regression analysis. For large values of b_B (corresponding to long echo times), the diffusion effect of slow-relaxing and relatively mobile water components leads again to a negative slope in the plot. This behavior corresponds qualitatively quite well to that shown in the simulations in figure 5. Under such conditions, no meaningful diffusion coefficients can be extracted from the echo ratio data any more.

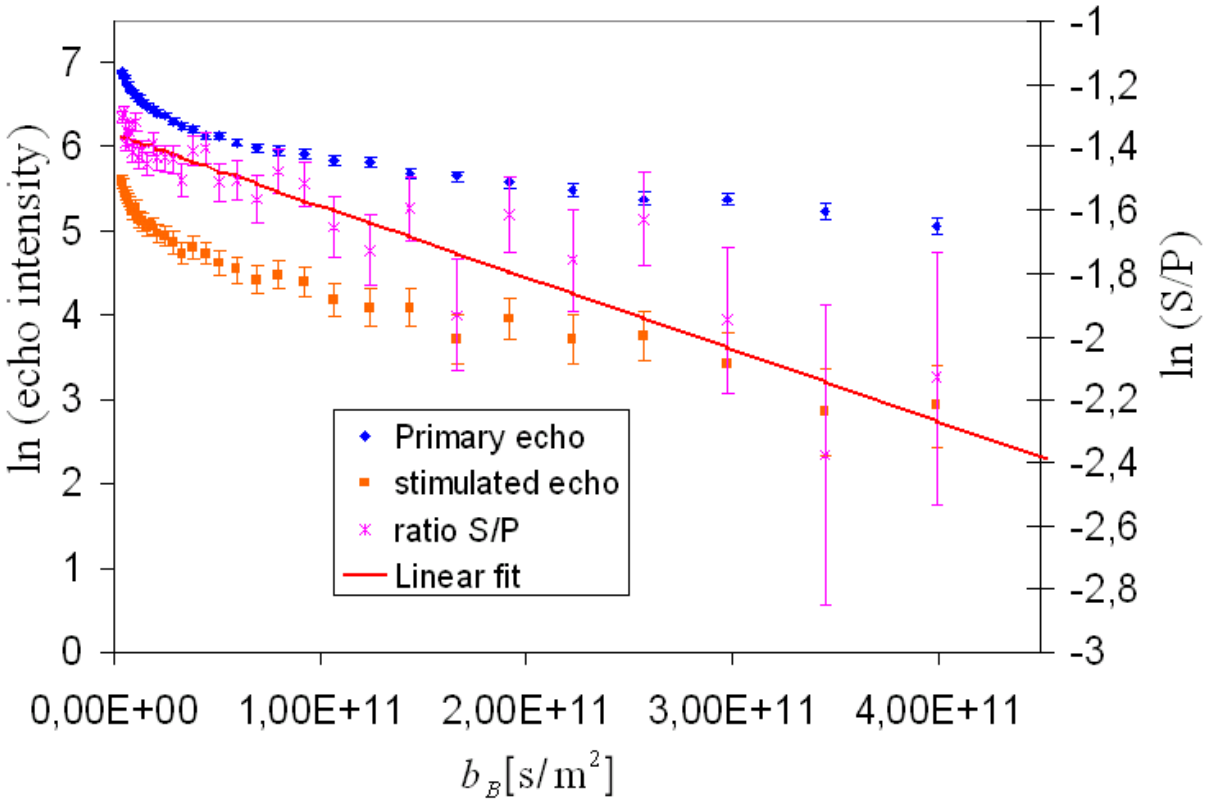

Fig. 9: Primary and stimulated echo signals and ratio of the echoes in an SFG diffusometry experiment on a white cement sample with w/c 0.25 after 34 h of hydration. The slope determined from the fit shown in the figure leads to a water self-diffusion coefficient of $(2.27\pm0.25)\times10^{-12}\mathrm{m^2/s}$.

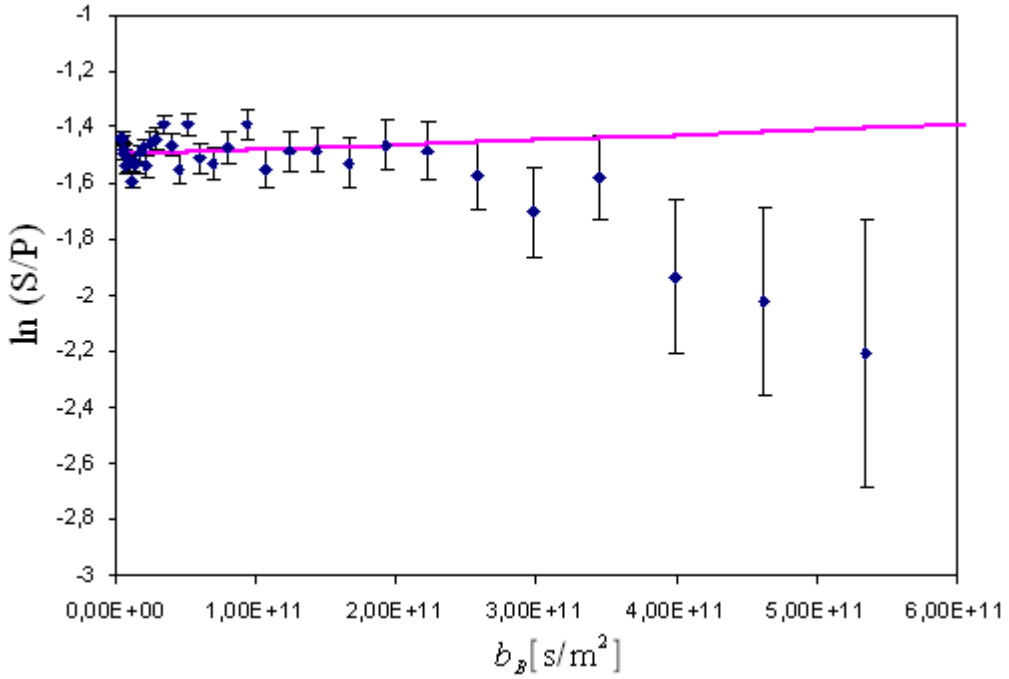

Fig. 10: S/P-Ratio in a SFG diffusometry experiment on the same white cement sample as in fig. 7 but after 4.5 days of hydration. While the initial data points show no clear trend and even a slightly positive slope (which makes physically no sense), there is a systematic bending to higher diffusive attenuation at the longer echo times which are not any more affected by the contribution of the fastest-relaxing water fraction in the material.

Short longitudinal relaxation times on the order of a few ms are quite common in hydrating cement [25,26]. Furthermore, some recent studies have shown that there is roughly a linear correlation between transverse and longitudinal relaxation times in cements after a few days of hydration [26]. As the relaxation time distribution in the hydrating cement moves more and more to a combination of short T_1 and T_2, artifacts of the kind shown in fig. 10 tend to disturb the diffusion measurement more and more. In the case of Dyckerhoff weiß at a w/c of 0.25, this problem was found to be relevant after about 3 days of hydration. In an Aquila Bianco sample with w/c 0.18, diffusion studies by the SFG proved possible even after 14 days of hydration (see fig. 11). This is in good accordance with observations in other NMR studies in which we found much longer relaxation times for the Aquila Bianco cement than for comparable mixtures of the Dyckerhoff weiß [17].

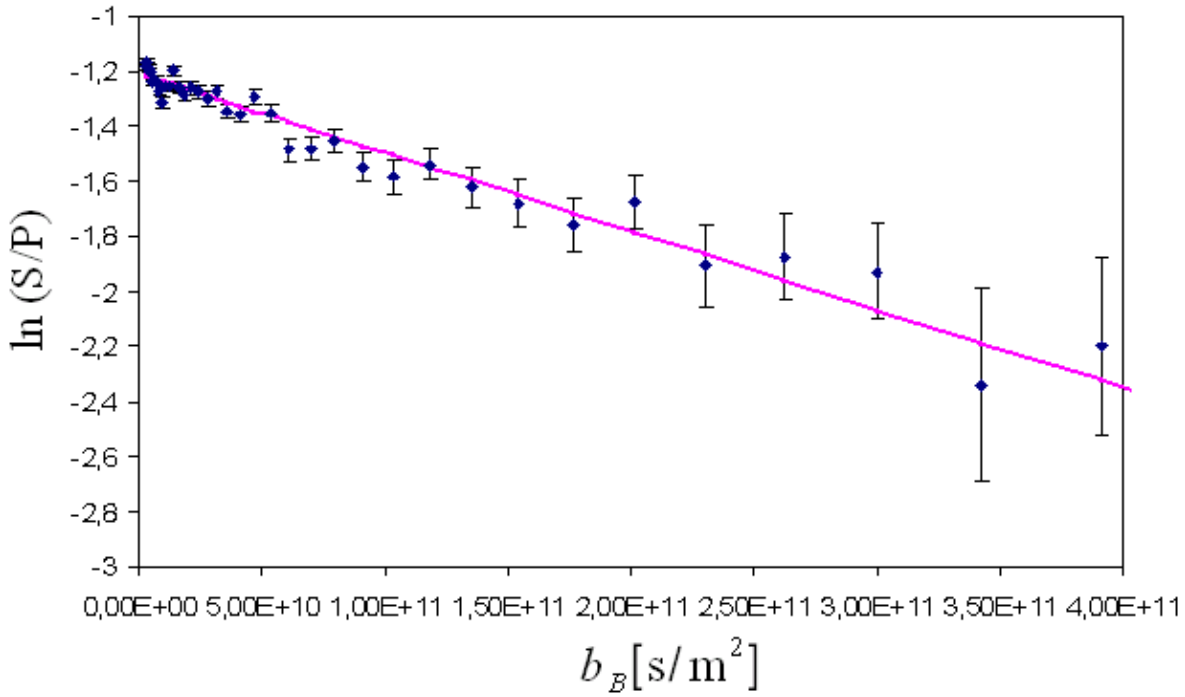

Fig. 11: Evaluation of the S/P-Ratio in an SFG diffusometry experiment on a white cement sample prepared from "Aquila Bianco" CEM I 32.5 R at a w/c of 0.18 (sample hydrated for 14 days, diffusion time t = 3 ms). The diffusion coefficient determined from the slope is $(2.85\pm0.5)\times10^{-12}\mathrm{m^2/s}$.

5.Conclusion and outlook

As the calculations and results in this paper demonstrate, the echo ratio approach to SFG NMR is beneficial to separate relaxation and diffusion effects in homogeneous materials. In complex materials such as hydrating cement however, the quite complex relaxation time weighting effects on the term presented in eqn. 7 may lead to seriously distorted diffusion coefficients. In applying the SFG echo ratio method to such samples, one has to carefully check for possible effects of this combined effect of T_1- and T_2-weighting which is most detrimental for sample components with a combination of a small diffusion coefficient, a short T_2 and a T_1 shorter or comparable to the diffusion time.

Despite all those caveats, the results presented in this paper demonstrate that the use of SFG NMR can extend the window of applicability of NMR diffusometry on hydrating cement samples to later hydration times and smaller self-diffusion coefficients.

In addition to the relaxation time weighting effects, also the different range of b_B values covered in SFG and PFG must be considered. The large range of b_B values in the SFG

experiment is especially necessary due to the intrinsically low signal/noise ratio of the SFG experiment in its conventional form [13] with its quite low "signal filling factor" (see figure 12).

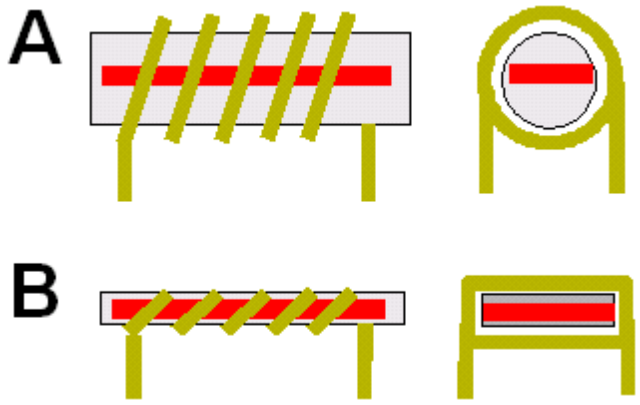

Fig. 12 "Signal filling factor" in SFG NMR experiments: sample volume (gray) and excited sample slice (red) (A) in a standard solenoidal coil (B) in a flattened solenoidal coil.

Substantial improvements of the signal/noise ratio of the SFG experiment can be expected in the future by the development of SFG NMR setups with an increased "signal filling factor" by using optimized coil geometries such as the flattened solenoidal coil sketched in figure 12B. Such efforts are under way at our lab in the context of another project [14].

References

[1] Callaghan, PT 1991 Principles of Magnetic Resonance Microscopy. Oxford, Clarendon Press.
[2] E. Hahn Physical Review 80 (1950) 580-594.
[3] J.H. Simpson, H.Y Carr, Physical Review 111 (1958) 1201-1202.
[4] E.O. Stejskal, J.E. Tanner, Journal of Chemical Physics 42 (1965) 288-292.
[5] J.E. Tanner, Journal of Chemical Physics 52 (1970) 2523-2526.
[6] W.S. Price, Concepts in Magnetic Resonance 9 (1997) 299-336.
[7] W.S. Price, Concepts in Magnetic Resonance 10 (1997) 197-237.
[8] F. Stallmach, J. Kärger, Adsorption 5 (1999) 117-133.
[9] N. Nestle, P. Galvosas, J. Kärger, Cem. Concr. Res. (2006) in press.
[10] F. Stallmach, P. Galvosas, Spin echo NMR diffusion studies Annu. Rep. NMR Spectrosc 61 (2007) 51-131.
[11] M. Holz, S.R. Heil, A. Sacco, Physical Chemistry Chemical Physics 2 (2000) 4740-4742.
[12] D. LeBihan, J.F. Mangin, C. Poupon, C.A.Clark, S. Pappata, N. Molko, H. Chabriat, J.Magn. Reson. Imaging 2001 13 (2001) 534–546.
[13] Chang, F. Fujara, B. Geil, G. Hinze, H. Sillescu, A. Tölle, J. Non-Cryst. Sol. 172-174 (1994) 674.
[14] A. Gädke, N. Nestle, Diffusion Fundamentals 3 (2005) 38.1 - 38.12.
[15] http://www.fkp.physik.tu-darmstadt.de/damaris/
[16] P. Galvosas, F. Stallmach, G. Seiffert, J. Kärger, U. Kaess, G. Majer, Journal of Magnetic Resonance 151 (2001) 260-268.
[17] N. Nestle, P. Galvosas, O. Geier, C. Zimmermann, M. Dakkouri, J. Kärger, Journal of applied Physics 89 (2001) 8061-8065.
[18] R.M. Cotts, M.J.R. Hoch, T. Sun, J.T. Markert, Journal of Magnetic Resonance 83 (1989) 252-266.

[19] N. Nestle, A. Qadan, P. Galvosas, W. Süss, J. Kärger Magnetic Resonance Imaging 20 (2002) 567-573.
[20] R. Blinc, M. Burgar, G. Lahajnar, M. Rozmarin, V. Rutar, I. Kocuvan , J. Ursic, Journal of the American Ceramic Society 61 (1978) 35-37.
[21] E.W. Hansen, H.C. Gran, E Johannessen, Microporous and Mesoporous Materials 78 (2005) 43-52.
[22] Teresa Nunes, E W Randall, A A Samoilenko, P Bodart, G Feio, J. Phys. D: Appl. Phys. 29 (1996) 805–808.
[23] H.J.P. Brocken, O.C.G. Adan, L. Pel, HERON 42 (1997) 55-69.
[24] S. Bejaoui, B. Bary, Cement and Concrete Research, in press.
[25] N. Nestle, C. Zimmermann, M. Dakkouri, J. Kärger, Journal of Physics D – Applied Physics 35 (2002) 166-171.
[26] P.J. McDonald, J.P. Korb, J. Mitchell, L. Montheilhet, Physical Review E 72 (2005) DOI:0011409.